Supporting Information

Dinitrosyliron Complex $[Fe_4(\mu_3\text{-}S)_2(\mu_2\text{-}NO)_2(NO)_6]^{2-}$ Containing Bridging Nitroxyls: ^{15}N (NO) NMR Analysis of the Bridging and Terminal NO-Coordinate Ligands

By

Shih-Wey Yeh, Chih-Chin Tsou, Wen-Feng Liaw*

Department of Chemistry and Frontier Research Center on Fundamental and Applied Sciences of Matters, National Tsing Hua University, Hsinchu 30013, Taiwan

E-mail: wfliaw@mx.nthu.edu.tw

Experimental Section

Manipulations, reactions, and transfers were conducted under nitrogen according to Schlenk techniques or in a glovebox (nitrogen gas). Solvents were distilled under nitrogen from appropriate drying agents (MeCN from CaH_2; hexane, diethyl ether and tetrahydrofuran (THF) from sodium and benzophenone) and stored in dried, N_2-filled flasks over 4 Å molecular sieves. Nitrogen was purged through these solvents before use. Solvent was transferred to the reaction vessel via stainless cannula under positive pressure of N_2. The reagents $NaNO_2$ (SHOWA), $Fe(CO)_5$ (Strem Chemicals), Tetramethylethylenediamine (TMEDA, Alfa Aesar), $[Cp_2Fe][BF_4]$, $HSCPh_3$ (Aldrich), 18-crown-6-ether (TCI) and $Na^{15}NO_2$ (ISOTEC) were used as received. Compounds $[(TMEDA)Fe(NO)_2]$, $[K\text{-}18\text{-}crown\text{-}6\text{-}ether]_2[Fe_2(\mu\text{-}S)_2(NO)_4]$ and $[PPN]_2[S_5Fe(\mu\text{-}S)_2FeS_5]$ were synthesized by published procedures.[1] Infrared spectra of the ν_{NO} stretching frequencies were recorded on a

PerkinElmer model spectrum One B spectrometer with sealed solution cells (0.1 mm, KBr and CaF_2 windows). UV–vis spectra were recorded on a Jasco V-570 spectrometer. ^{15}N NMR spectra were acquired on a BRUKER AVANCE DMX 600 NMR spectrometer. ^{15}N NMR spectra were recorded at 60.702 MHz. Chemical shifts (δ) of ^{15}N NMR are relative to neat 1 M $Na^{15}NO_2$ in D_2O (δ 232 ppm) as the external standard.[2] Analyses of carbon, hydrogen, and nitrogen were obtained with a CHN analyzer (Heraeus).

Preparation of [K-18-crown-6-ether]$_2$[Fe$_4$(μ_3-S)$_2$(μ_2-NO)$_2$(NO)$_6$] (1). The $\{Fe(NO)_2\}^{10}$ DNIC [(TMEDA)Fe(NO)$_2$] (0.046 g, 0.2 mmol) and RRS [K-18-crown-6-ether]$_2$[Fe$_2$(μ-S)$_2$(NO)$_4$] (0.09 g, 0.1 mmol) were dissolved in CH_3CN (10 mL) at ambient temperature. After the mixture solution was stirred for 20 min at room temperature, the reaction was monitored by FTIR. The IR ν_{NO} stretching frequencies (1742 w, 1701 s and 1668 m cm^{-1} (CH_3CN)) were assigned to the formation of [K-18-crown-6-ether]$_2$[Fe$_4$(μ_3-S)$_2$(μ_2-NO)$_2$(NO)$_6$] (**1**). The addition of diethyl ether to the resulting solution led to precipitation of dark brown solid (yield 0.092 g, 86 %). Diffusion of diethyl ether into the CH_3CN solution of complex **1** at room temperature led to dark brown crystals suitable for single-crystal X-ray diffraction. IR ν_{NO}: 1742 w, 1701 s and 1668 m cm^{-1} (CH_3CN); 1739 w, 1702 sh, 1685 vs, 1668 s and 1510 m cm^{-1} (KBr). Absorption spectrum (CH_3CN): 273 (4725), 343 (2697) and 478 (1301) nm. Anal. Calcd for $C_{24}H_{48}Fe_4K_2N_8O_{20}S_2 \cdot 2CH_3CN$: C, 27.65; H, 4.47; N, 11.51. Found: C, 27.52; H, 4.48; N, 11.52.

Reaction of Complex 1, [Cp$_2$Fe][BF$_4$] and HSCPh$_3$. Under N_2 atmosphere, complex **1** (0.113 g, 0.1 mmol), [Cp$_2$Fe][BF$_4$] (0.027 g, 0.1 mmol) and $HSCPh_3$ (0.028 g, 0.1 mmol) were loaded in a tube, and then placed in a larger tube containing a THF-CH_3CN solution of [PPN]$_2$[S$_5$Fe(μ-S)$_2$FeS$_5$] (0.039 g, 0.025 mmol). The larger tube was then capped with a well-sealed septum. CH_3CN was added via cannula into the small tube containing complex **1**, [Cp$_2$Fe][BF$_4$] and $HSCPh_3$ and then the mixture solution was stirred for 12 h at room temperature. The resulting green solution in the larger vial was transferred to Schlenk tube

and dried under vacuum. The dark-green crude solid was redissolved in THF and filtered through Celite to remove the insoluble solid. Addition of hexane to the filtrate led to precipitation of the known dark-green solid [PPN][$S_5Fe(NO)_2$] (62%), characterized by IR spectrum.[1c] At the same time, the resulting solution produced in the inner tube was monitored by IR ν_{NO} 1796 w, 1741 s and 1706 w cm^{-1} (CH_3CN), consistent with the formation of the known [K-18-crown-6-ether][$Fe_4(\mu_3\text{-}S)_3(NO)_7$] (RBS).[3] Addition of diethyl ether to the resulting solution led to precipitation of RBS (yield 0.077 g, 92 %) characterized by IR and UV-vis spectroscopy.

Magnetic Measurements. The magnetic data were recorded on SQUID magnetometer (SQUID-VSM Quantum Design Company) under 0.5 T external magnetic field in the temperature range 2–300 K. The magnetic susceptibility data were corrected with ligands' diamagnetism by the tabulated Pascal's constants.

Magnetic Susceptibility. The magnetic susceptibility values of powdered sample of complex **1** increase from 1.847×10^{-4} cm^3 mol^{-1} at 300 K to 2.531×10^{-3} cm^3 mol^{-1} at 2 K (SI Figure S2). The effective magnetic moment values decrease from 0.666 μ_B at 300 K to 0.201 μ_B at 2 K (SI Figure S2). The corresponding $\chi_M T$ values decrease from 5.55×10^{-2} cm^3 K mol^{-1} at 300 K to 5.06×10^{-3} cm^3 K mol^{-1} at 2 K (SI Figure S3). Bleaney and Bowers' equation $\chi_M = (2Ng^2\beta^2/kT)/[3+\exp(\Delta_{S/T}/kT)]$, where $\Delta_{S/T}$ is the singlet/triplet (S/T) energy splitting ($\Delta_{S/T} = E_{S=1} - E_{S=0}$),[4] describes the covalent delocalization between two [$\{Fe(NO)_2\}^9$-$\{Fe(NO)_2\}^{10}$] motifs, leading to the ground state S = 0. In order to get the best fit of the SQUID data, the Hamiltonian ($\hat{H} = 2g\beta\hat{S}H$) was used to describe two uncoupled S = 1/2 radicals (spin-only value $\chi_M T$ = 0.75 cm^3 K mol^{-1}).[5] As shown below, fitting of the magnetic data is based on the assumption of the presence of two [$\{Fe(NO)_2\}^9$-$\{Fe(NO)_2\}^{10}$] motifs and uncoupled S = 1/2 diradicals (or decomposition species).

$\chi_M^{exp} = (1 - p)\,\chi_M\{2[\{Fe(NO)_2\}^9\text{-}\{Fe(NO)_2\}^{10}]\} + p\,\chi_M$ (uncoupled S = 1/2 diradicals) + TIP

The best fit of the experimental data to the resonance hybrid model gives $g([\{Fe(NO)_2\}^9\text{-}\{Fe(NO)_2\}^{10}]) = 1.997$, $\Delta_{S/T} = 1843 \pm 2$ cm^{-1}, $\theta = -4.53 \pm 0.94$ K, p = 1.76 % and TIP = $(141.6 \pm 3.3) \times 10^{-6}$ cm^3 mol^{-1} with $R^2 = 0.991$ (SI Figure S3).

Crystallography. Crystallographic data of complex **1** were summarized in Supplementary Information Table S2. The crystal chosen for X-ray diffraction studies measured 0.41 × 0.33 × 0.11 mm^3 for complex **1**. Crystal was mounted on a glass fiber and quickly coated in epoxy resin. Unit-cell parameters were obtained by least-squares refinement. Diffraction measurements for complex **1** was carried out on a SMART CCD (Nonius Kappa CCD) diffractometer with graphite-monochromated Mo K_α radiation (λ = 0.71073 Å) and between 1.76 and 25.06˚ for complex **1**. Least-squares refinement of the positional and anisotropic thermal parameters of all non-hydrogen atoms and fixed hydrogen atoms was based on F^2. A SADABS absorption correction was made.[6] The SHELXTL structure refinement program was employed.[7] CCDC-974703 (complex **1**) contains the supplementary crystallographic data for this paper. These data can be obtained free of charge from The Cambridge Crystallographic Data Centre via www.ccdc.cam.ac.uk/data_request/cif.

Computational Details. All DFT calculations were performed on the *Gaussian 09* program.[8] All geometry optimizations were conducted with DFT using the BP86 functional[9] and a mixed basis set of SDD ECP[10] on Fe and 6-311++G(d,p)[11] on all other atoms. The methodology was chosen because it has been shown to have good accuracy for DNIC system.[12] For solvent correction a PCM model with aceton (ε = 20.493) was applied in the conformations **A-^{15}NO** and **B-^{15}NO**.[13] Frequency calculations were carried out for detected stationary points to ensure that they correspond to either true minima on the potential energy hypersurface. The thermal correction to Gibbs free energy was made under the conditions of 220 K and 1 atm (or 298.15 K and 1 atm).

References

1. (a) M.-C. Hung, M.-C. Tsai, G.-H. Lee and W.-F. Liaw, *Inorg. Chem.* 2006, **45**, 6041–6047. (b) A. R. Butler, C. Glidewell and M. H. Li, *Adv. Inorg. Chem.* 1988, **32**, 335−393. (c) M.-L. Tsai, C.-C. Chen, I.-J. Hsu, S.-C. Ke, C.-H. Hsieh, K.-A. Chiang, G.-H. Lee, Y. Wang and W.-F. Liaw, *Inorg. Chem.* 2004, **43**, 5159–5167.
2. (a) J. Mason, D. M. P. Mingos, D. Sherman and R. W. M. Wardle, *J. Chem. Soc., Chem. Commun.* 1984, 1223–1225. (b) J. Mason, L. F. Larkworthy and E. A. Moore, *Chem. Rev.* 2002, **102**, 913–934.
3. A. R. Butler, C. Glidewell, A. R. Hyde and J. C. Walton, *Polyhedron* 1985, **4**, 797–809.
4. P. Chen, D. E. Root, C. Campochiaro, K. Fujisawa and E. I. Solomon, *J. Am. Chem. Soc.* 2003, **125**, 466−474.
5. O. Kahn, *Molecular Magnetism*; VCH Publishers: New York, 1993; pp 103−107.
6. G. M. Sheldrick, *SADABS*; University of Göttingen: Göttingen, Germany, 1996.
7. G. M. Sheldrick, *SHELXTL*; Siemens Analytical X-ray InstrumentsInc.: Madison, WI, 1994.
8. M. J. Frisch, G. W. Trucks, H. B. Schlegel, G. E. Scuseria, M. A. Robb, J. R. Cheeseman, J. A. Jr. Montgomery, T. Vreven, K. N. Kudin, J. C. Burant, J. M. Millam, S. S. Iyengar, J. Tomasi, V. Barone, B. Mennucci, M. Cossi, G. Scalmani, N. Rega, G. A. Petersson, H. Nakatsuji, M. Hada, M. Ehara, K. Toyota, R. Fukuda, J. Hasegawa, M. Ishida, T. Nakajima, Y. Honda, O. Kitao, H. Nakai, M. Klene, X. Li, J. E. Knox, H. P. Hratchian, J. B. Cross, V. Bakken, C. Adamo, J. Jaramillo, R. Gomperts, R. E. Stratmann, O. Yazyev, A. J. Austin, R. Cammi, C. Pomelli, J. W. Ochterski, P. Y. Ayala, K. Morokuma, G. A. Voth, P. Salvador, J. J. Dannenberg, V. G. Zakrzewski, S. Dapprich, A. D. Daniels, M. C. Strain, O. Farkas, D. K. Malick, A. D. Rabuck, K. Raghavachari, J. B. Foresman, J. V. Ortiz, Q. Cui, A. G. Baboul, S. Clifford, J. Cioslowski, B. B. Stefanov, G. Liu, A. Liashenko, P. Piskorz, I. Komaromi, R. L. Martin,

D. J. Fox, T. Keith, M. A. Al-Laham, C. Y. Peng, A. Nanayakkara, M. Challacombe, P. M. G. Gill, B. Johnson, W. Chen, M. W. Wong, C. Gonzalez and J. A. Pople, Gaussian 09.

9. (a) A. D. Becke, *Phys. Rev. A* 1988, **38**, 3098−3100. (b) J. P. Perdew, *Phys. Rev. B* 1986, **33**, 8822−8824.
10. M. Kaupp, P. V. R. Schleyer, H. Stoll and H. Preuss, *J. Chem. Phys.* 1991, **94**, 1360−1366.
11. (a) R. Krishnan, J. S. Binkley, R. Seeger and J. A. Pople, *J. Chem. Phys.* 1980, **72**, 650−654. (b) A. J. H. Wachters, *J. Chem. Phys.* 1970, **52**, 1033−1036. (c) P. J. Hay, *J. Chem. Phys.* 1977, **66**, 4377−4384.
12. S. M. Brothers, M. Y. Darensbourg and M. B. Hall, *Inorg. Chem.* 2011, **50**, 8532−8540.
13. S. Miertus, E. Scrocco and J. Tomasi, *Chem. Phys.* 1981, **55**, 117−129.

Table S1. Selected experimental and computational geometry parameters and NO vibrational frequencies.

Parameter	Complex **1**	**Ladder-form A**	**Boat-form B**
Fe(1)···Fe(2) (Å)	2.573(1)	2.583	2.585
Fe(1)···Fe(1^{i}) (Å)	2.740(1)	2.692	2.693
Fe(1)-N(1), N(1)-O(1) (Å)	1.660(3), 1.184(4)	1.635, 1.198	1.638, 1.202
Fe(1)-N(2), N(2)-O(2) (Å)	1.761(3), 1.224(4)	1.741, 1.218	1.743, 1.216
Fe(2)-N(2) (Å)	1.967(3)	1.972	1.964
Fe(2)-N(3), N(3)-O(3) (Å) **Fe(2)-N(4), N(4)-O(4) (Å)**	1.676(4), 1.182(5) 1.663(4), 1.181(4)	1.649, 1.201 1.638, 1.204	1.649, 1.197 1.639, 1.205
Fe(1)-S(1)-Fe(2) (°)	69.6(1)	69.9	70.2
Fe(1)-N(2)-Fe(2) (°)	87.1(1)	88.0	88.2
N(1)-Fe(1)-N(2) (°)	106.5(2)	109.4	110.0
N(3)-Fe(2)-N(4) (°)	117.4(2)	112.6	112.1
Fe(1)-N(1)-O(1) (°)	170.2(3)	173.5	172.3
Fe(1)-N(2)-O(2) (°)	138.8(3)	140.2	140.2
Fe(2)-N(2)-O(2) (°)	131.0(3)	128.9	129.2
Fe(2)-N(3)-O(3) (°) **Fe(2)-N(4)-O(4)** (°)	166.7(3) 171.5(3)	161.2 168.5	161.5 167.0
νNO (cm^{-1})	1739 w, 1702 sh, 1685 vs, 1668 s, 1510 m	1696 s, 1682 s, 1645 m, 1533 m	1726 w, 1682 s, 1678 s, 1667 s, 1645 m, 1540 w, 1538 m

Table S2. Crystal data and structure refinement for complex **1**.

Identification code	ch15230	
Empirical formula	C24 H48 Fe4 K2 N8 O20 S2	
Formula weight	1134.42	
Temperature	200(2) K	
Wavelength	0.71073 Å	
Crystal system	Triclinic	
Space group	$P\bar{1}$	
Unit cell dimensions	a = 9.479(2) Å	α= 99.547(4)°.
	b = 11.160(2) Å	β= 109.035(3)°.
	c = 12.966(3) Å	γ = 113.002(3)°.
Volume	1123.7(4) $Å^3$	
Z	1	
Density (calculated)	1.676 Mg/m^3	
Absorption coefficient	1.623 mm^{-1}	
F(000)	582	
Crystal size	0.41 x 0.33 x 0.11 mm^3	
Theta range for data collection	1.76 to 25.06°.	
Index ranges	-11<=h<=11, -13<=k<=12, -15<=l<=15	
Reflections collected	9349	
Independent reflections	3956 [R(int) = 0.0344]	
Completeness to theta = 25.06°	99.0 %	
Absorption correction	multi-scan	
Max. and min. transmission	0.8417 and 0.5558	
Refinement method	Full-matrix least-squares on F^2	
Data / restraints / parameters	3956 / 0 / 271	
Goodness-of-fit on F^2	1.070	
Final R indices [I>2sigma(I)]	R1 = 0.0408, wR2 = 0.1175	
R indices (all data)	R1 = 0.0578, wR2 = 0.1486	
Largest diff. peak and hole	0.878 and -0.805 $e.Å^{-3}$	

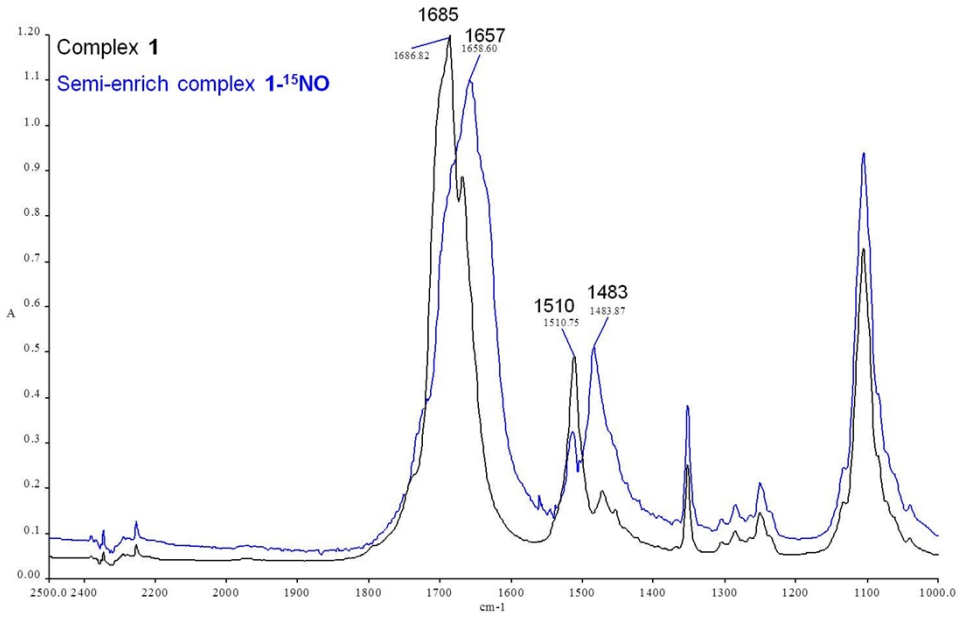

Figure S1. The solid-state infrared spectra of complex **1** (black line) and semi-enriched complex **1-^{15}NO** (blue line) mixed with KBr, respectively.

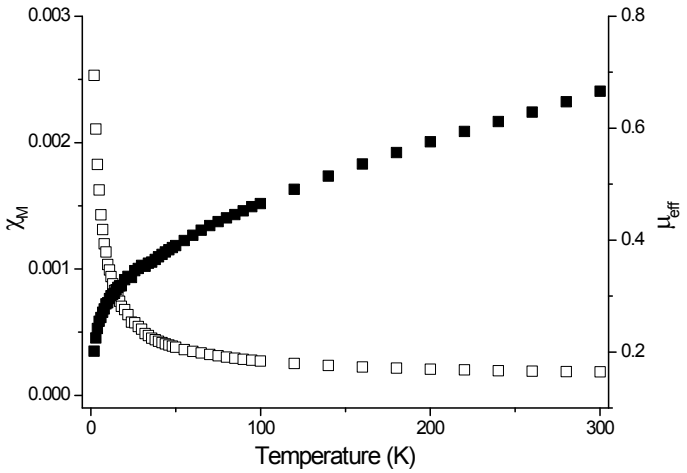

Figure S2. (a) The magnetic susceptibility of complex **1** under 0.5 T applied field (□□□), and (b) effective magnetic moment (μ_{eff}) vs temperature (T) plot (■■■).

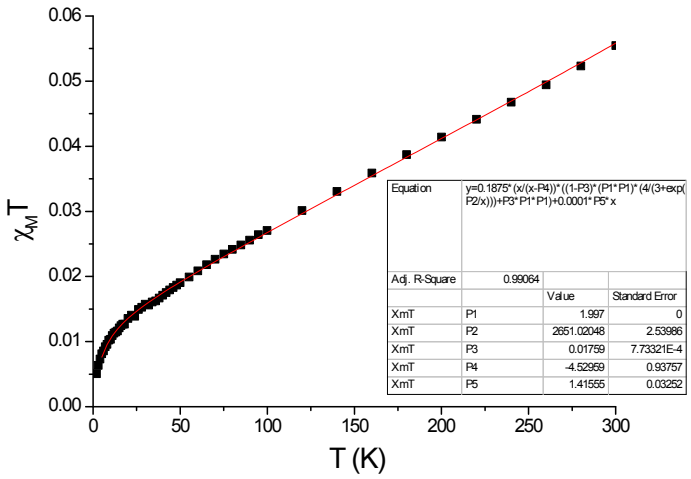

Figure S3. The plot of $\chi_M T$ vs. temperature for complex **1** under 0.5 T applied field and the best fit (red line) gives g([{Fe(NO)$_2$}^{9}-{Fe(NO)$_2$}^{10}) = 1.997, $\Delta_{S/T}$ = 1843 ± 2 cm^{-1}, θ = – 4.53 ± 0.94 K, p = 1.76 % and TIP = (141.6 ± 3.3) · 10^{-6} cm^3 mol^{-1} (R^2 = 0.991).

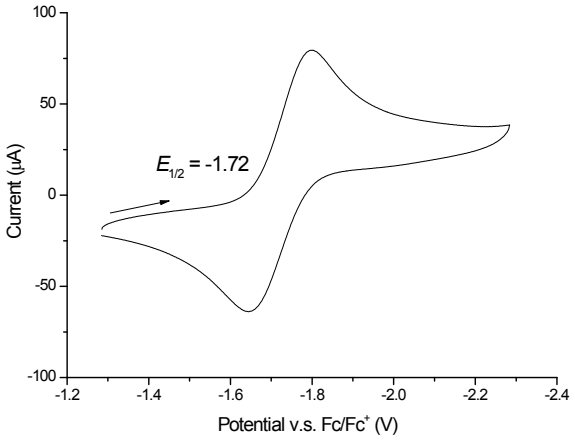

Figure S4. Cyclic voltammogram of complex **1** in a 2.5 mM CH_3CN solution with 0.1 M [^{n}Bu$_4$N][PF$_6$] as supporting electrolyte at room temperature, scan rate 0.5 V/s.

(a) 1726 w cm^{-1}

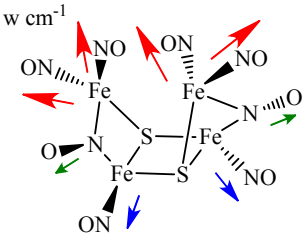

(b) 1682 s cm^{-1}

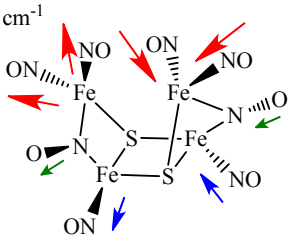

(c) 1678 s cm^{-1}

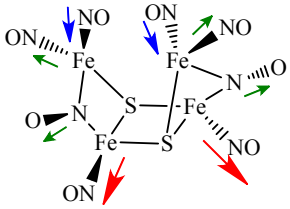

(d) 1667 s cm^{-1}

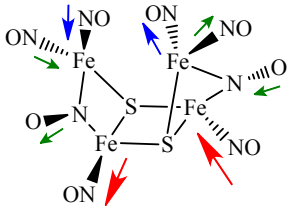

(e) 1645 m cm^{-1}

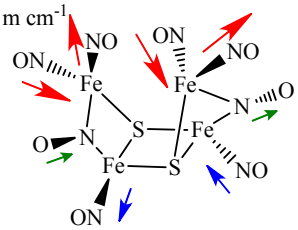

(f) 1540 w cm^{-1}

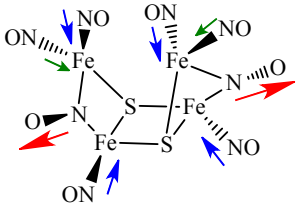

(g) 1538 m cm^{-1}

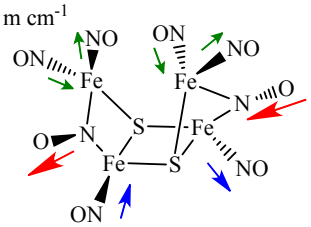

Chart S1. NO vibrational modes of boat-form **B**. The calculated IR spectrum of comformation **B** displays seven active NO vibrational frequencies at 1726, 1682, 1678, 1667, 1645, 1540 and 1538 cm^{-1}, which mainly correspond to (a) the two symmetric stretching vibration of two $\{Fe(NO)_2\}$ motifs, (b, e) the two anti-symmetric stretching vibrations of two $\{Fe(NO)_2\}$ motifs, (c) the symmetric stretching vibration of two central Fe-terminal NO motifs, (d) the anti-symmetric stretching vibration of two central Fe-terminal NO motifs, (f) the symmetric stretching vibration of two Fe_2-semibridging NO motifs, and (g) the anti-symmetric stretching vibration of two Fe_2-semibridging NO motifs, respectively.